Development of Acrylic PSA with LDH Nanocomposites: Synthesis, Characterization and Performance Evaluation

Shivraj J. Dhole¹, Tushar D. Deshpande¹, Jitendra S. Narkhede¹*

¹University Institute of Chemical Technology, Kavayitri Bahinabai Chaudhari North Maharashtra University, Jalgaon-425001, Maharashtra, India.

*Corresponding Author: Jitendra S. Narkhede

.....

Abstract: In the present study, acrylic-based PSAs (pressure-sensitive adhesives) have been developed using a solution polymerization process, employing 2-ethylhexyl acrylate in combination with vinyl terminated polydimethylsiloxane (PDMS) and acrylic acid, with benzoyl peroxide serving as the radical initiator. To enhance the adhesive performance, layered double hydroxide (LDH) nanoparticles were incorporated at concentrations amounts between 0.1 to 0.9 weight percent (wt%), resulting in PSA-LDH nanocomposites. The fourier transform infrared spectroscopy (FTIR) employing attenuated overall reflectivity was used to track the polymerization process, while the adhesive properties were evaluated through standard tack, peel, and adhesive tests.

The research results indicated that the incorporation for LDH significantly enhanced the adhesive tensile strength on wood substrates and enhanced the rheological behavior measured via a rheometer. Notably, the formulation containing 0.5 wt% LDH exhibited the highest improvements in tack and maximum load-bearing capacity compared to the unmodified PSA (0% LDH). Furthermore, amplitude sweep analysis and viscosity measurements indicated that LDH incorporation increased the structural complexity of the PSA matrix. All prepared nanocomposite formulations exhibited good stability under ambient storage conditions.

Key-words: pressure sensitive adhesive, tensile strength, Tack test, amplitude sweeps analysis.

1. Introduction

Pressure-sensitive adhesives (PSAs) are viscoelastic polymers capable of adhering to a wide range of surfaces both metallic and non-metallic through the application of slight pressure and brief contact time [1]. Their performance is generally defined by three key attributes: tack, peel strength, and shear resistance. Together, these properties govern the versatility of PSAs in practical applications. For an effective PSA, the ratio of storage modulus at higher frequencies to that at lower frequencies must be relatively large [2]. Acrylic-based PSAs are usually formulated using a combination of hard and soft monomers, initiators, and functional additives. Their adhesion behavior depends on factors such as the ability of the adhesive to flow and wet the substrate (which enhances tack), Since these parameters jointly determine adhesive strength, achieving simultaneous improvement in tack, peel, and shear adhesion continues to be a challenge, particularly for latex-based PSA systems [3]. Typically, acrylate-based systems consist of three categories of monomers: (i) low-glass-transition-temperature monomers that impart tackiness, (ii) high-glass-transition-temperature monomers that provide cohesion, and (iii) functional monomers that enable modification [4]. Various strategies have been explored to optimize PSA properties, such as Chain transfer agents (CTAs) are incorporated. However, these approaches often affect the adhesive characteristics unevenly.

The use of nanomaterials has emerged as another promising route, leading to the development of PSA nanocomposites with superior performance. Nanofillers including carbon nanotubes, nanoclay, nanosilica, and TiO₂ nanoparticles have been shown to enhance thermal stability, modulus, and mechanical strength in PSA systems [5]. Polymer nanocomposites in general are attractive for adhesive applications because they can offer improved modulus, higher thermal resistance, reduced gas permeability, and lower flammability. Two common methods for preparing solvent-based nanocomposite adhesives are (i) direct blending of nanoparticle dispersions with PSA solutions or latexes, and (ii) in situ synthesis during polymerization [6]. Among these, blending is the simplest and most widely applied, as it enables straightforward control over polymer properties during processing [7].

Nanofillers with plate-like structures are of growing interest due to their efficiency in reinforcing PSA matrices. Inorganic nanoparticles with different morphologies spherical, tubular, or platelet-shaped have been incorporated into adhesives, showing potential for structural and functional improvements. LDHs, or layered double hydroxides, are a type of anionic clay, are a notable class of such two-dimensional nanomaterials [8]. Their chemical formula can be expressed as $[M^{2+}_{1-x} M^{3+}_{x} (OH)_{2}]^{-} (A^{n-})_{x/n} mH_{2}O$, where M^{2+} and M^{3+}

represent trivalent and divalent cations, respectively; x corresponds to the molar fraction of the trivalent ion; and Aⁿ⁻ denotes the interlayer anion. LDHs are highly versatile because of their ability to intercalate functional species, exfoliate within polymer matrices, and hybridize with other nanomaterials. Consequently, they have been explored in diverse areas such as catalysis, electrochemistry, and drug delivery [9].

The present work introduces an approach of developing nanocomposites by dispersing exfoliated LDH nanoplatelets in a solvent based acrylic copolymer based on acrylic acid, 2-ethylhexyl acrylate (2-EHA) and vinyl terminated polydimethylsiloxane. The study systematically investigates how varying LDH filler concentrations influence viscoelastic and adhesive performance, with a particular focus on changes in molecular structure. Results reveal that incorporating 0.5 wt% of LDH nanoplatelets produces an optimized composite formulation, leading to marked enhancements in tack, adhesive strength, viscoelastic behavior, and overall adhesion performance.

2. Materials and methods

2.1 | Materials:

The monomers utilized in the process included 2-ethylhexyl acrylate (2-EHA, procured from Sigma-Aldrich) and acrylic acid (sourced from Merck Chemicals, Mumbai, India). Vinyl terminated polydimethylsiloxane (PDMS) was supplied by Sigma-Aldrich. Ethyl acetate, purchased from Merck Chemicals, was used as the reaction solvent. Benzoyl peroxide, obtained from Molychem, Mumbai, functioned as the free-radical initiator in the polymerization process. the Layered double hydroxide (LDH) which is used as a reinforcing nanofiller was purchased from the Sigma-Aldrich distributor in Nagpur, India.

2.2 Methods:

2.2.1 Synthesis of acrylic PSA by solution polymerization:

The acrylic pressure-sensitive adhesive (PSA) was synthesized via solution polymerization, employing ethyl acetate as the reaction medium and benzoyl peroxide (BPO) as the free-radical initiator. In a typical procedure, ethyl acetate was charged into a 250 mL round-bottom flask, where it functioned as a solvent to regulate viscosity, facilitate heat dissipation, and ensure uniform temperature control throughout the reaction. Subsequently, a monomeric mixture constructed from 2-ethylhexyl acrylate (2-EHA), vinyl terminated polydimethylsiloxane (PDMS), and acrylic acid (AA) in a 2:0.5:1 weight ratio was introduced into the reactor, after which 0.2 g of BPO was added.

At 80 °C, the polymerization process was conducted under a continuous nitrogen (N₂) atmosphere to maintain inert conditions and suppress premature termination. The reaction progressed for approximately 5 h, during which the viscosity gradually increased as polymer chains formed alongside residual unreacted monomers. Upon completion, After cooling to room temperature, the reaction mixture was put into glass containers. The obtained polymeric solution displayed viscoelastic characteristics, indicative of the successful formation of the PSA matrix. Figure 1 shows a schematic illustration of the synthetic pathway.

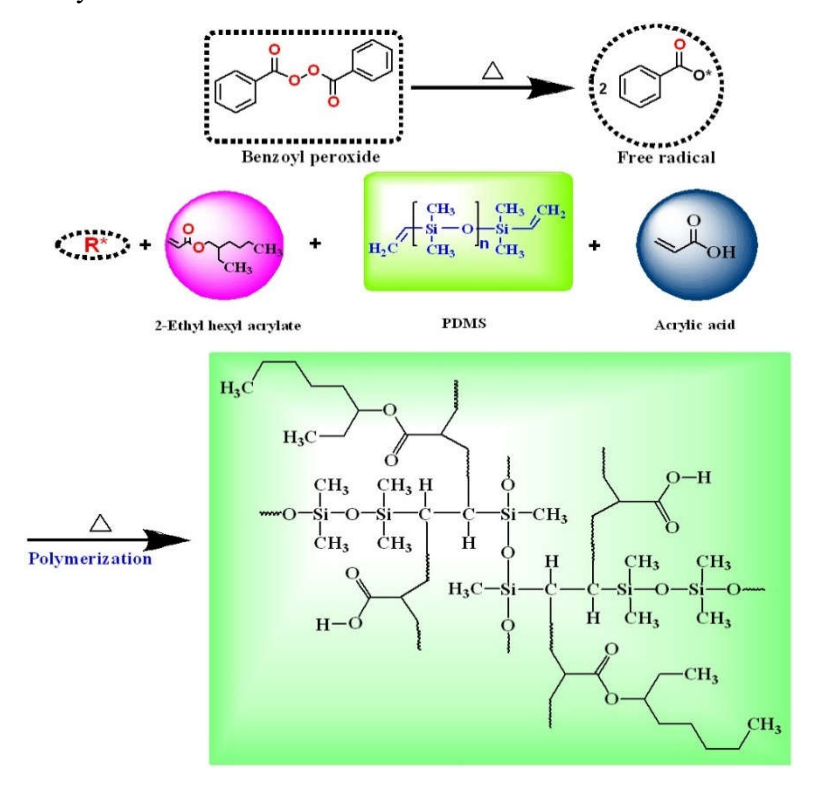


Figure 1. The Scheme of Synthesis of Solvent-Based Pressure Sensitive

Adhesive

2.2.2 Preparation of PSA with LDH Nanocomposite:

Analytical-grade layered double hydroxide (LDH) nanoplatelets, with an average particle size of 10–30 nm, were dispersed in ethyl acetate (EA) and subjected to ultrasonic exfoliation using a tip sonicator operating at 360 W with a pulse sequence of 1s ON and 6s OFF for 1 h. To prevent thermal degradation during sonication, the beaker was immersed in a cold-water bath. The resulting LDH dispersion was then incorporated into the acrylic pressure-sensitive adhesive (PSA) under continuous mechanical stirring at ambient temperature for 45 min, yielding nanocomposites with LDH concentrations ranging from 0.1 to 0.9 wt% relative to polymer content. The obtained PSA/LDH suspensions

demonstrated long-term stability, with no observable nanoparticle sedimentation over several months. The nanocomposite adhesives were subsequently applied onto different substrates, including wood, glass, and PVC back sheets, using conventional laboratory coating and joining procedures [10]. Among these, wood substrates exhibited the highest adhesion strength, and therefore, adhesive strength analysis was primarily focused on wood samples. Mechanical performance of the PSA/LDH formulations was evaluated using universal testing machine (UTM), providing comprehensive insights into their adhesive and structural characteristics.

2.3 Characterization:

For characterizing the adhesive performance of the produced PSAs, following test methods were used:

2.3.1 Fourier Transform Infra-Red Spectroscopy:

Utilizing Fourier-transform infrared (FTIR) spectroscopy, the chemical composition and interfacial structural characteristics of the acrylic adhesives were examined, both in the absence and presence of LDH fillers. Measurements were carried out using a Shimadzu (Japan) spectrometer performing in the 400–4000 cm⁻¹ spectral region and fitted with an attenuated total reflectance (ATR) accessory [11].

2.3.2 Differential scanning calorimetry:

Utilizing differential scanning calorimetry (DSC), the thermal characteristics of PSA samples and LDH nanoplatelets was investigated, both unmodified and LDH-reinforced. The measurements were conducted on a Hitachi DSC-7020 instrument. The specimens (5–10 mg) were accurately weighed, sealed in aluminium pans, and subjected to analysis in a dry nitrogen environment at a flow rate of 60 mL/min , 20 °C/min heating ramp from –50 °C to 350 °C.

2.3.3 Thermogravimetric analysis:

The thermal properties of solvent-based acrylic PSAs were evaluated using thermogravimetric analysis (TGA) and their nanocomposite counterparts reinforced with LDH nanoplatelets. The measurements were carried out on a TGA-55 instrument (TA Instruments, Denmark) under a nitrogen atmosphere. Samples were heated from 30 °C to 700 °C to evaluate their thermal degradation behavior [12].

2.3.4 High-resolution transmission electron microscopy:

Transmission electron microscopy with high resolution (HR-TEM, Technai-20, Philips, Holland) was employed to examine the dispersion state of LDH nanoplatelets. For sample preparation, carbon-coated copper grids were pretreated with 2% (w/v) phosphotungstic acid then subsequently air-dried. The specimens were then imaged at an accelerating voltage of 200 kV, and micrographs were recorded on varying magnifications to evaluate nanoplatelet morphology and distribution [13].

2.3.5 Adhesive characteristics:

The adhesive performance was evaluated on multiple substrates, including aluminium, PVC sheets, wood, and mild steel. Among these, wood exhibited the highest bonding strength; therefore, subsequent adhesive strength investigations were carried out on wood specimens. Single-lap joint samples were fabricated in accordance with ASTM D2559 specifications for structural wood adhesives. Each wooden adherend measured 25.4 mm in width, 8 mm in thickness, also 80 mm in length, with an additional 20 mm designated for the overlap region [14]. The overlap area of both adherends was uniformly coated with the adhesive, and the assemblies were pressed together and cured at room temperature. After complete curing, the lap joints were subjected to shear tensile testing using a universal tensile testing machine (UTM, Hi-Tech Instruments, Mumbai). The shear strength values were determined from the load–displacement data obtained during testing.

2.3.6 Rheology and Tack test:

A rheometer (MCR-302, Anton Paar, Graz, Austria) with a parallel plate shape was used to analyze the viscoelastic characteristics of the PSA formulations. Frequency sweep experiments were carried out at 25 °C. Throughout the 0.01–100 rad/s oscillation frequency range under controlled stress conditions. To evaluate the materials' elastic and viscous contributions, the storage modulus (G') and loss modulus (G'') were measured as functions of frequency at room temperature [15]. Tack performance was evaluated by means of the probe-tack method in accordance with ASTM D2979-95. In this test, a flat-ended cylindrical steel probe (5.0 mm diameter) was exposed to a specific pressure of 10 kPa for about one second when in contact with the PSA film. The probe was then withdrawn at a controlled rate, and the maximum detachment force was recorded, representing the tack strength of the adhesive.

2.3.7 Peel Adhesion Testing:

Measurements of peel strength were made at room temperature to assess the adhesion of the prepared PSA films. Adhesive tapes were cut to dimensions of 1 × 12.7 cm and applied onto clean glass plates, followed by a resting period of 20 min prior to testing. The free end of the adhesive strip was clamped horizontally in the upper grip of the testing machine, and the glass plate was fastened in the lower grip. Peel tests were carried out at a 180° angle with a speed of 300 mm/min across the head. The peel adherence of the PSA on the glass substrate was measured using the force that was recorded during detachment.

3. Result and Discussion

3.1 Fourier transform infrared spectroscopy:

FTIR (Fourier transform infrared) spectroscopy was used to look at the molecular structure and confirm a chemical composition of the prepared acrylate-based pressure-sensitive adhesives (PSAs). Figure 2(a) illustrates the spectra of five representative formulations: PSA (0% LDH) and LDH-modified PSAs containing 0.1%, 0.3%, 0.5%, 0.7%, and 0.9% LDH by weight. All spectra displayed a series of common absorption bands, reflecting the characteristic functional groups originating from the acrylate monomers. A strong band observed near 2950 cm⁻¹ corresponds to the Si–CH₃ stretching vibration, confirming the presence of alkyl side groups within the polymer matrix [16]. The stretching vibration of the carbonyl (C=O) group is responsible for the absorption peak at 1720 cm⁻¹. Which is a signature of acrylic acid [17]. Additional deformation vibrations were also detected, including the CH₃ bending mode at 1368 cm⁻¹ [18]. The prominent C–O stretching bands appearing at 1013 and 1158 cm⁻¹ further validate the successful copolymerization of acrylate monomers [19].

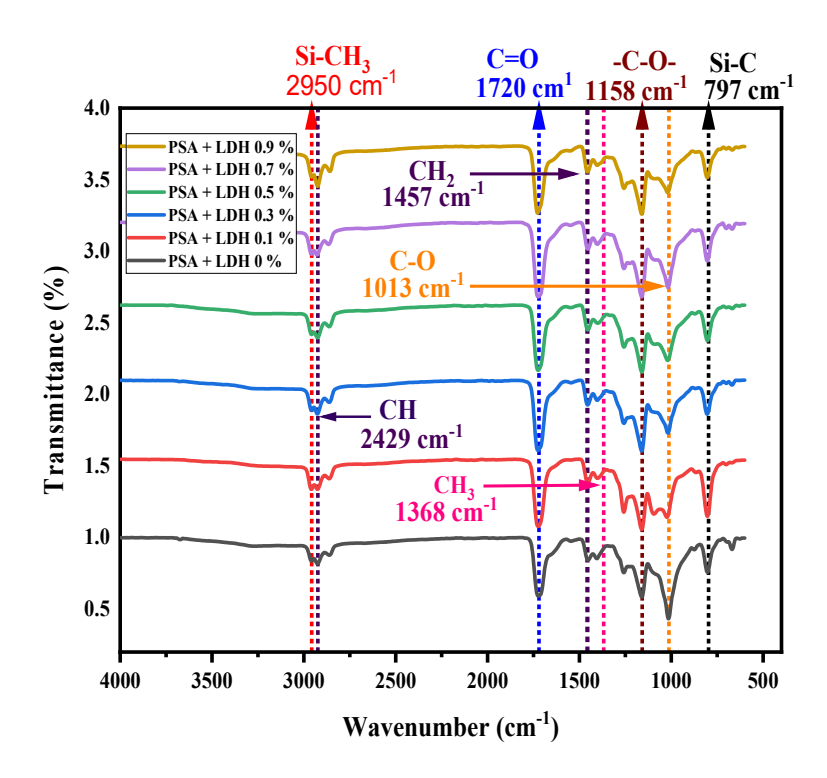


Figure 2(a). FTIR spectrum of acrylate-based PSA with varying concentration of LDH NPs

Interestingly, the CH₂ stretching band around 2429 cm⁻¹ showed enhanced intensity, suggesting a higher degree of acrylic acid and ethyl acrylate incorporation within the PSA backbone. At 1640 cm⁻¹, the absence of absorption signifies the full consumption of vinyl double bonds during polymerization, confirming the efficient conversion of monomers into the copolymer network.

The FTIR spectra of Mg–Al layered double hydroxide (LDH) are presented in figure 2(b). LDH belongs to the hydrotalcite family, characterized as an anionic clay where interlayer anions maintain equilibrium between the positively charged brucite-like layers. These structural features generate distinctive vibrational modes in the IR region. Typically, the primary absorption bands for hydrotalcites appear in the 400–800 cm⁻¹ range, a value consistent for the octahedral sheets' metal–oxygen (M–O) bonds' bending and stretching vibrations. Absorption peaks around 654 cm⁻¹ and 776 cm⁻¹ were identified, assigned to Mg–O and Al–O stretching vibrations, confirming the presence of brucite-like layers [20]. Moreover, the spectrum of Mg–Al LDH–CO₃²- exhibits a wide OH stretching band with a noticeable shoulder that measures between 3300 and 3600 cm⁻¹ [21]. This characteristic results from hydrogen- bonding interactions among intercalated carbonate anions and the hydroxyl compounds found in the brucite layers. Compared with pure brucite, where the

OH stretching vibration occurs around 3550–3570 cm⁻¹, the shift to approximately 3431 cm⁻¹ in Mg–Al LDH indicates stronger hydrogen bonding [22].

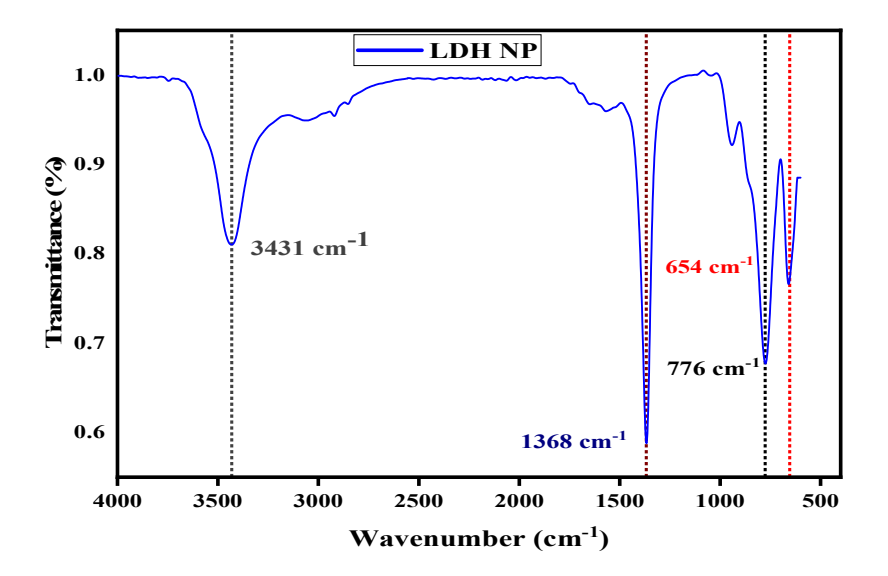


Figure 2(b). FTIR spectrum of LDH NPs.

3.2 Differential scanning calorimetry:

Utilizing differential scanning calorimetry (DSC), an effect of LDH incorporation on thermal transitions was examined. Figure 3 shows the DSC thermograms of neat PSA and PSA containing varying LDH loadings (0–0.5 wt.%). The primary thermal event observed for all samples is the glass transition (Tg), which reflects the onset of segmental mobility of the polymer chains.

The DSC analysis (Figure 3) revealed a systematic change with respect to PSA's glass-transition temperature (Tg) when LDH is added [23]. The neat PSA exhibited a Tg of –30.5 °C (-10 °C), representing the inherent chain mobility of the polymer matrix. With the addition of LDH the glass transition temperature shifts on lower side attributing to the localized chain immobilization at the LDH surface. PSA with 0.5 % LDH shows the glass transition temperature of -20 °C. The shift of glass transition temperature on lower side is due to the LDH nanosheets, disrupting polymer–polymer packing and introduced interfacial free volume, creating mobile interfacial zones and thereby enhancing chain mobility. This progressive Tg depression implies that LDH incorporation tunes the viscoelastic window of the PSA, with low to medium loadings favoring enhanced tack and wetting due to increased flexibility, while higher concentrations may compromise cohesive strength and thermal resistance because of excessive softening [24].

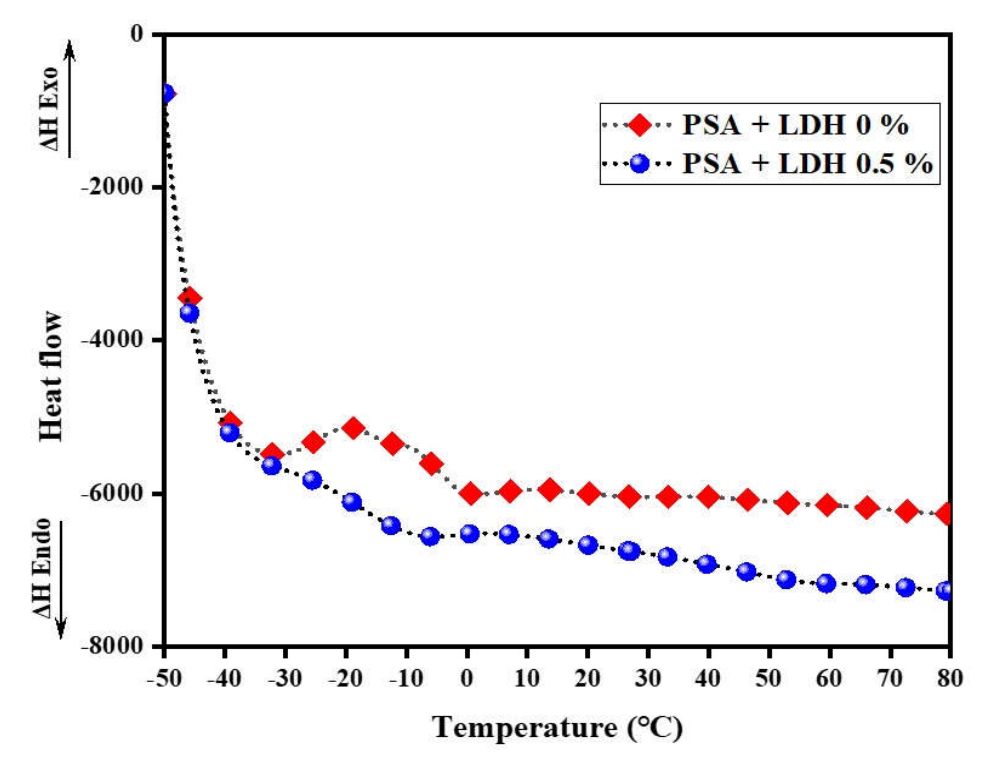


Figure 3: DSC spectra of pure PSA, and PSA with varying concentration of LDH NPs

3.3 Thermal Analysis of PSA and PSA with LDH Nanocomposites:

Thermogravimetric analysis (TGA), was carried out in order to evaluate thermal stability of solvent-based acrylic pressure-sensitive adhesives (PSA) and their nanocomposites reinforced with layered double hydroxide (LDH) nanoparticles, in an environment of nitrogen and between 30-600 °C. As shown in figure 4, all samples exhibited comparable thermal degradation patterns, with substantial mass loss caused on by the disintegration of polymer chains occurring at 183°C and 500°C.

The onset decomposition temperature (T_{onset}), defined at 0.5 wt% weight loss, increased from 189.3 °C for neat PSA to 211 °C upon incorporating 0.5 wt% LDH, indicating improved thermal stability. This enhancement is attributed to the well-dispersed LDH layers, which act as barriers, slowing down the escape of volatile degradation products. However, further increasing LDH content to 0.7 wt% and 0.9 wt% resulted in lower T_{onset} values of 198 °C and 194 °C, respectively. This decline in thermal performance at higher LDH loadings may be due to nanoparticle agglomeration and restacking, which hinder their dispersion and reduce their effectiveness [25].

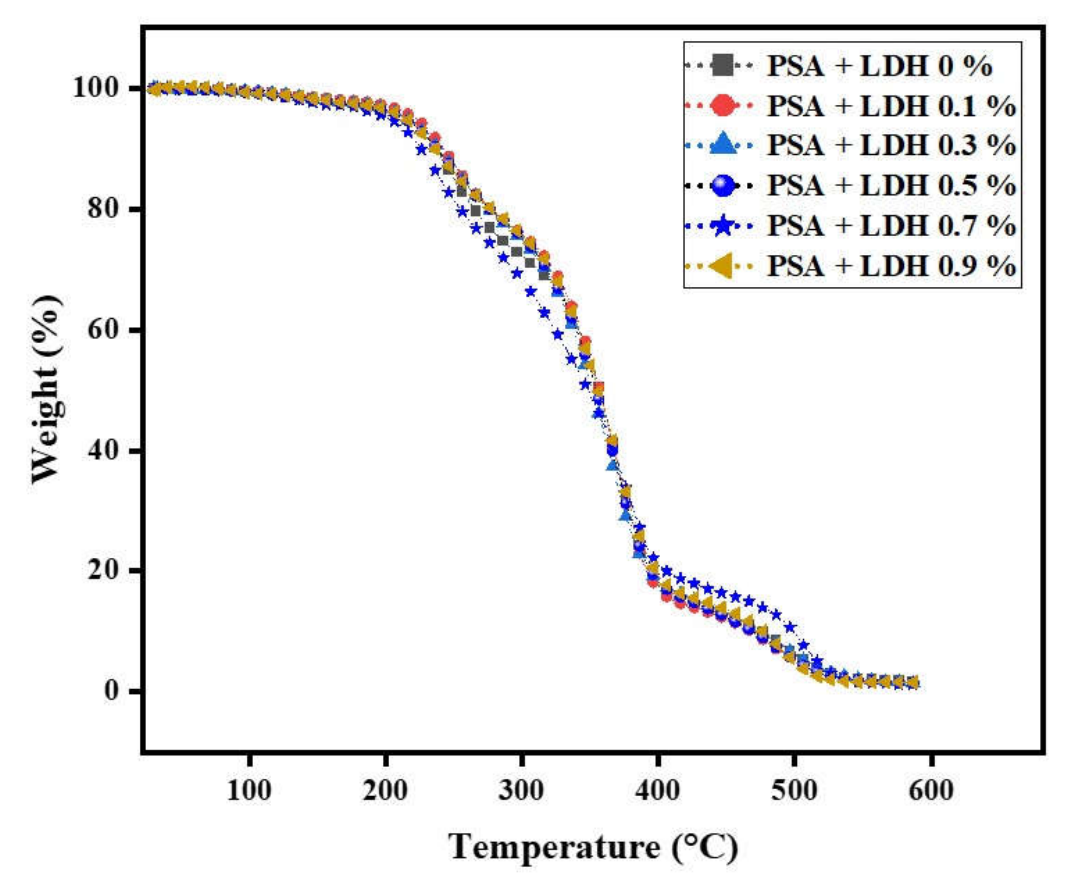


Figure 4. Thermogravimetric curve of pure PSA, LDH NPs, and PSA with varying concentration of LDH NPs

3.4 Morphology of nanoparticles and PSA formulations:

Analysis using transmission electron microscopy (TEM) was conducted with a high-resolution TEM (Technai-20, Phillips, Holland). Figure 5 presents the TEM micrographs of the exfoliated LDH nanoplatelets, evidently showing particles are composed of ultrathin two-dimensional layers. A significant fraction of the particles consists of only one or two stacked layers, while others are formed by a few molecular layers. The extremely thin morphology of LDH nanoplatelets makes them highly transparent to the incident electron beam, thereby enabling precise visualization of their structure [26]. This nanoscale size distribution contributes to their good dispersion and stability in ethyl acetate, which is beneficial for homogeneous mixing with the acrylic PSA matrix. Figure 5(a) displays the low-magnification HR-TEM image of exfoliated LDH nanoplatelets with a scale bar of 200 nm, whereas figure 5(b) depicts a high-magnification image with a 100 nm scale bar, offering more detailed insight into their layered structure.

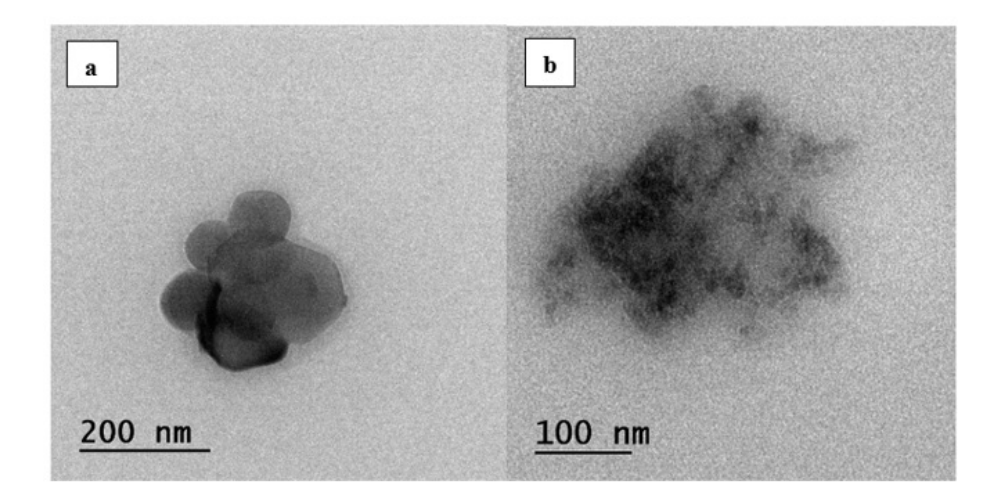


Figure 5. (a) The high-resolution transmission electron microscopic (HR-TEM) image of exfoliated LDH nanoplatelets at a lower magnification image with a scale bar of 200 nm and (b) a higher magnification image with a scale bar of 100 nm.

Furthermore, the microstructural morphology of PSA dispersions containing LDH was observed using an optical microscope (Leica DM750), as shown in figure 6 (a,b). These microscopic observations confirm the well-dispersed nature of LDH within the adhesive matrix, further supporting their suitability for enhancing the performance of PSA formulations.

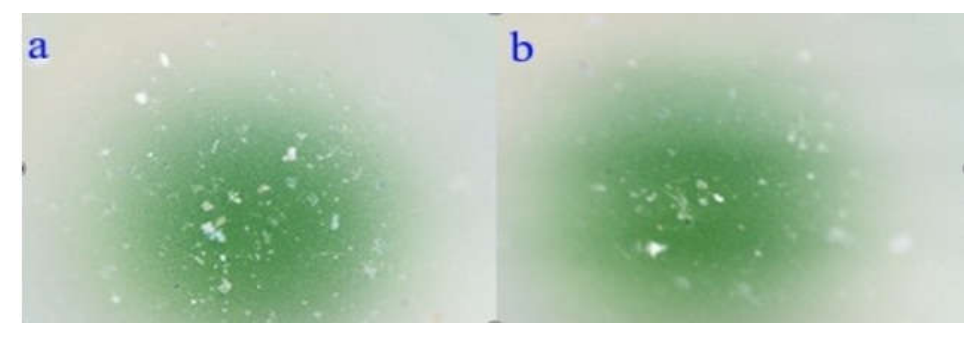


Figure 6. Microscopic image of PSA dispersion captured using Leica DM750 optical microscope

3.2 Adhesive Characteristic:

The prepared PSA joints were tested according to the lap joint method to get responses when applying displacement. Graphical curves with typical load displacement data for reinforced and unreinforced PSA with LDH NPs are presented in table 1. And depicted in figure 7. Additionally, a comparison is made between the average highest load values that were attained for the unreinforced and reinforced specimens with LDH.

Table 1 presents the load-bearing capacities of PSA samples with different LDH contents. The unreinforced PSA joint exhibited a maximum load of 7.15 Kg. However, a slightly higher load of 7.25 Kg was obtained when 0.1 wt% LDH was added. A substantial improvement was observed at 0.3 wt% and 0.5 wt% LDH, with load capacities of 19.65 kg and 61.85 kg, respectively. Beyond this point, a gradual decline was recorded, with 43.55 kg for 0.7 wt% LDH and 37.20 kg for 0.9 wt% LDH.

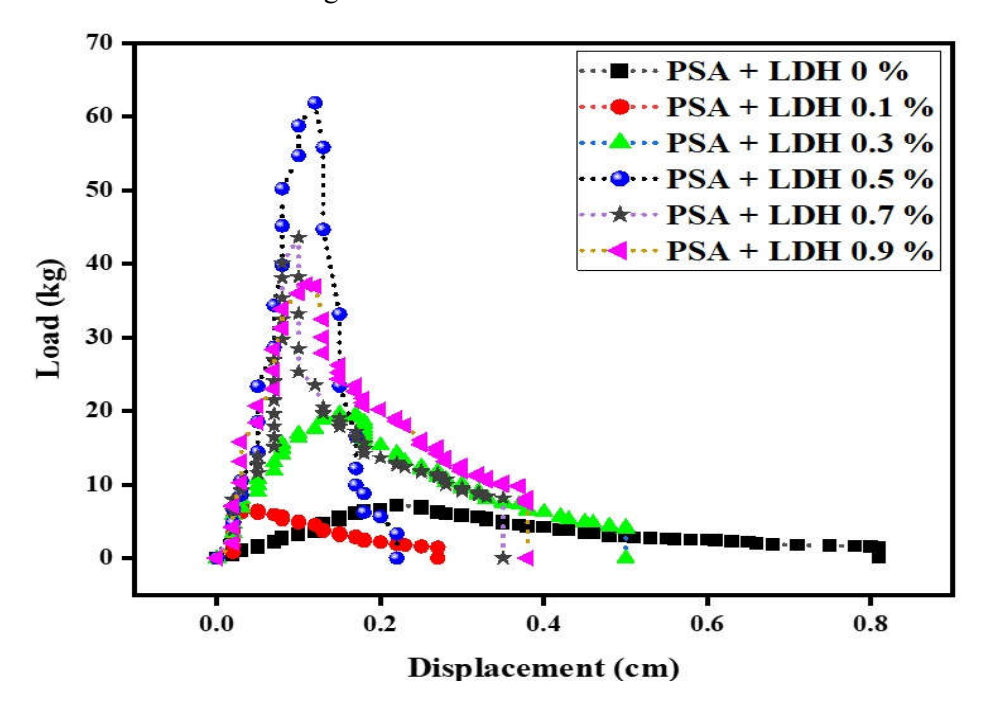


Figure 7. Load vs Displacement graph for Lap joint test.

Table 1. Peak Load Data of Reinforced and Unreinforced PSA For The Adhesive Tensile Test Using Lap Joint Test Method

	PSA+LDH					
Sample Name	0 %	0.1 %	0.3%	0.5 %	0.7 %	0.9 %
Load in Kg	7.15	7.25	19.65	61.85	43.55	37.2

The optimum performance was achieved at 0.5 wt% LDH, where the maximum load was 8.65-fold higher compared to the unreinforced PSA. This remarkable enhancement can be attributed to the extension and stabilization of the fibrillation plateau, leading to stronger and more stable fibril formation during deformation. However, further increases in LDH loading beyond 0.5 wt% resulted in a decline in adhesive properties, as excessive filler addition diminishes the energy dissipation ability of the PSA matrix [5].

Figure 8 presents the effect of LDH content on the peel strength of PSA samples. Except for the control specimen, all LDH-reinforced samples exhibited a noticeable increase in peel strength with rising LDH concentration. For the PSA + 0.5 wt% LDH sample, the maximum peel strength reached 1.5 kg/cm, showing a significant enhancement compared with the neat PSA. This improvement is attributed to the reduction in surface tension induced by LDH, which enhances adhesive wetting at the substrate interface. Increased wettability leads to stronger mechanical interlocking within surface imperfections and pores, thereby contributing to improved peel strength [27].

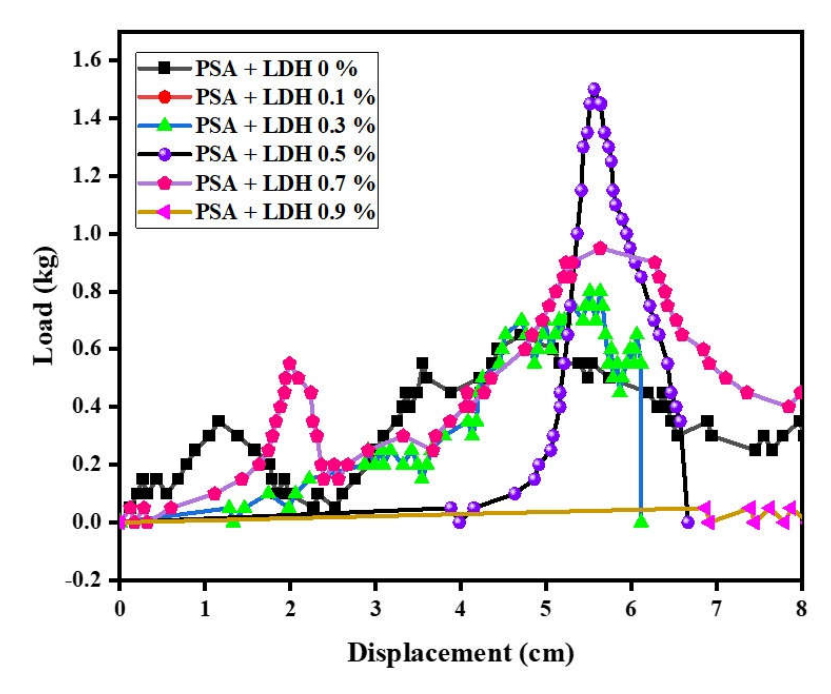


Figure 8. Variation of peel strength with LDH concentration for various PSA using 180° peel test.

3.6 Tack test

Tack or tackiness, in material science describes the intrinsic stickiness of a substance, which may originate from cohesive forces within the adhesive bridging two substrates, or adhesive forces at the interface between dissimilar surfaces. The test involves measuring the force required to separate two parallel plates having a defined volume of material between them from a stationary position with no initial pressure applied. The peak in negative normal force (tension) can be attributed to 'tack' and the area under the force-time curve to adhesive or cohesive strength. Tack test results as shown in figure 9 demonstrate the effect of LDH addition on PSA performance. The PSA sample containing 0.5 wt% LDH appears to be the tackiest of the studied formulations, exhibiting a remarkable 11.37-fold increase in tack performance comparative to the neat PSA (unreinforced). In terms of the area under the curves, which relates to

adhesive/cohesive strength, the PSA sample containing 0.5 wt% LDH appears to be strongest. However, the force decay profiles are almost similar for all formulations. The strength of adhesive bonding is influenced by several thermodynamic interactions, including hydrogen bonding across the interface, electrostatic attractions, and van der Waals interactions.

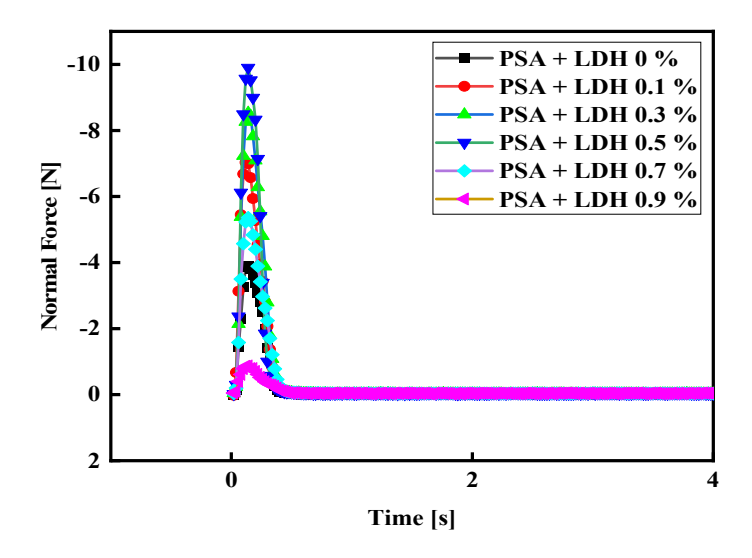


Figure 9. Tack force versus time graph for PSA samples

Furthermore, rheological factors contribute significantly, as viscoelastic energy dissipation during polymer chain deformation within the adhesive layer directly impacts the work of adhesion in tack testing [28]. This viscoelastic contribution is reflected in the loop tack forces recorded for PSAs containing different LDH loadings.

3.7 Rheological analysis of PSA with LDH NPs:

The amplitude sweep test is an essential rheological analysis used to establish the Linear Viscoelastic Region (LVER), which defines the stability of a material within a specific strain range. The rheological behavior of solvent-based pressure sensitive adhesive (PSA) composites incorporating varying concentrations of layered double hydroxide (LDH) nanoparticles was systematically investigated to elucidate their viscoelastic properties and flow characteristics. The dynamic storage modulus (G') and loss modulus (G") were found to be significantly reliant upon both the shear strain and LDH concentration, according to amplitude sweep experiments. Figure 10 represents the amplitude sweep profiles of PSA and PSA samples reinforced with varying concentrations of LDH nanoplatelets (0.1–0.9 wt%). The unmodified PSA does not show crossover points

between G' and G" indicating its solid like nature. At a shear strain of approximately 0.5%, the pure PSA undergoes structural breakdown and transitions into a flow state. For the PSA + 0.1 wt% LDH system, the rheological profile suggests that the overall network structure is not significantly altered; however, the modulus values are higher compared to the unreinforced PSA, indicating enhanced stiffness [29]. In contrast, The PSA samples having 0.3, 0.5, 0.7, and 0.9 wt% LDH consistently demonstrate G' values higher than G", signifying the material behaves in a solid-like manner, dominating the viscous properties throughout the tested strain range. The absence of crossover points in these systems reflects improved stability within the applied shear strain window. Such distinct separation between G' and G" demonstrates that the composites maintain a consistent rheological character.

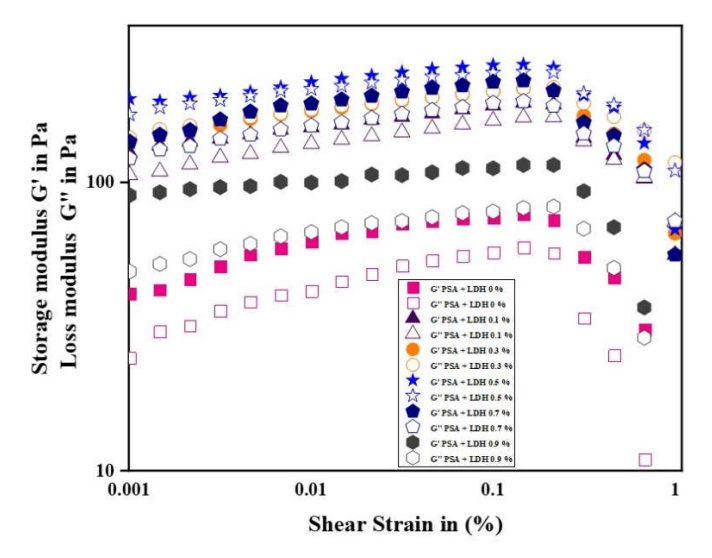


Figure 10. Amplitude sweep test results illustrating the variation of the dynamic storage modulus (G') and loss modulus (G") with shear strain (γ) for PSA, and PSA with varying concentration of LDH NPs.

For all PSA samples, G' remained greater than G" in The region of linear viscoelasticity, which shows primarily elastic properties, while modulus coefficients increased with higher LDH loading, highlighting enhanced network structure and mechanical reinforcement due to nanoparticle incorporation [30].

Viscosity, which measures resistance to deformation, was evaluated across shear rates around 0.1 to 100 s⁻¹. The figure 11 shows flow curve analysis demonstrating shear-thinning behavior across all samples. The addition of LDH nanoparticles shows increased zero shear viscosity, which drops with increasing shear rate, where increasing shear induces molecular rearrangements that reduce resistance to flow with the 0.5% LDH loading the

most pronounced effect on initial viscosity is noticed, suggesting improved particle—polymer interactions and stronger interfacial adhesion [31].

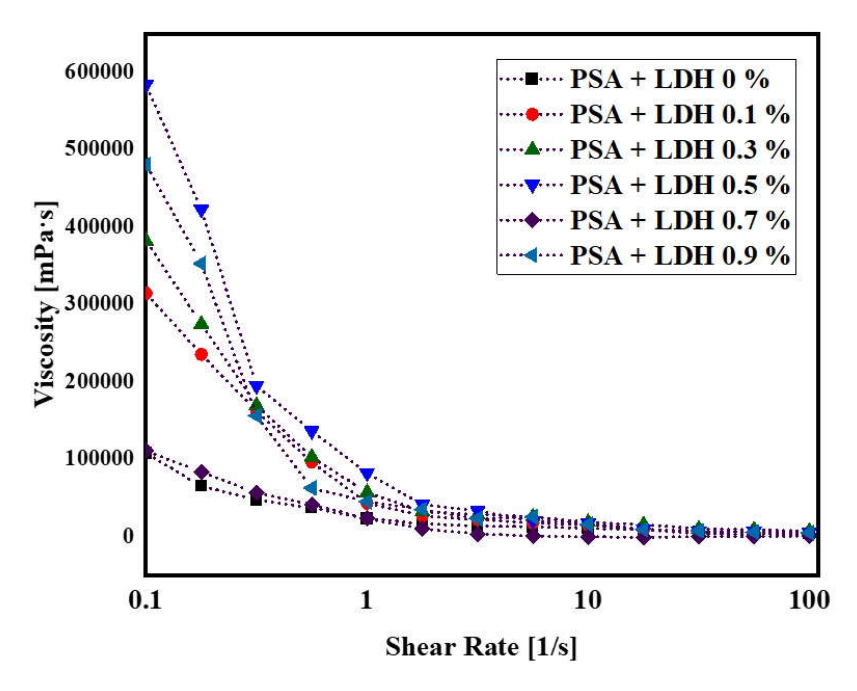


Figure 11. Flow curve plot of viscosity vs. shear rate for PSA samples

The $\tan \delta$ parameter, representing the damping capacity of the adhesive, provides insights into its ability to dissipate energy [32]. Figure 12 shows that increasing LDH content enhances the damping properties of PSA. Importantly, this effect persists across all concentrations, with $\tan \delta$ values rising progressively with higher LDH loadings. The $\tan \delta$ (G"/G') analysis further corroborated these findings, where lower $\tan \delta$ values at low shear strains indicated a transition toward more solid-like behavior with increasing LDH concentration, reinforcing the structural integrity of the PSA.

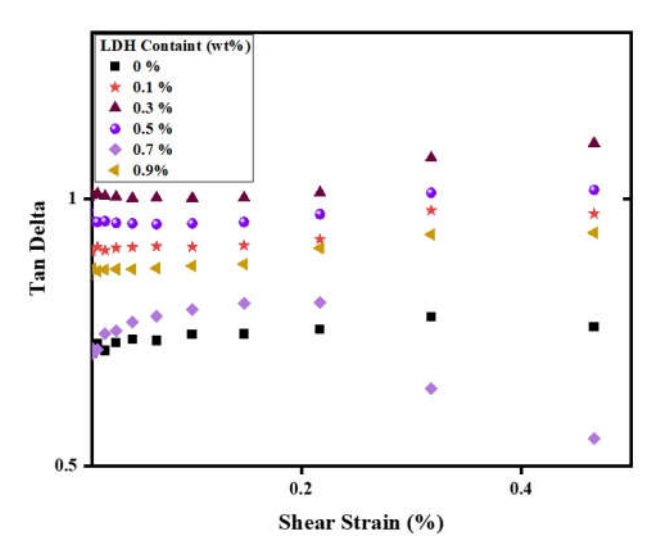


Figure 12: Shear strain vs tan delta graph of PSA samples.

These results confirm that the inclusion of LDH nanoparticles significantly modifies the rheological profile of the PSA system, which is critical for tailoring adhesive performance in applications demanding high mechanical strength and stability under dynamic stress conditions.

4. Conclusion

In this investigation, efforts were directed toward improving the effectiveness of an acrylic pressure-sensitive adhesive (PSA) based on solvents by incorporating layered double hydroxide (LDH) nanoparticles. The adhesive matrix was synthesized via solution polymerization employing a solvent of ethyl acetate, with acrylic acid (AA), vinyl terminated polydimethylsiloxane (PDMS) and 2-ethylhexyl acrylate (2-EHA) as the monomers. Notable improvements in thermal and adhesive properties were observed following LDH incorporation.

Mechanical testing of lap-shear joints demonstrated that PSA containing 0.5 wt% LDH achieved the highest maximum load, corresponding to an 8.65-fold increase relative to the neat PSA.

Tack evaluation revealed a remarkable 11.37 fold improvement in the PSA + 0.5% LDH sample, highlighting the significant enhancement in surface stickiness. Rheological characterization, including amplitude sweep and viscosity assessments, indicated that blending LDH with the PSA matrix introduced greater structural complexity. The PSA + 0.5% LDH formulation showed a higher viscosity and storage modulus, pointing toward stronger network interactions. All samples exhibited shear-thinning behavior, with viscosity decreasing under increasing shear, yet LDH incorporation consistently raised viscosity across the tested concentrations.

Tan delta analysis provided further insights, demonstrating that LDH addition increased the damping ability of the PSA. Moreover, a continuous rise in damping was recorded with increasing LDH content, while stability under varying shear strain was maintained.

In conclusion, the incorporation of LDH nanoparticles into acrylic PSAs resulted in a nanocomposite adhesive with markedly enhanced adhesion strength, viscoelastic performance, and overall functionality. These advancements highlight the potential of LDH-reinforced PSAs for high-performance and multifunctional adhesive applications.

Reference

- [1] M. Zhu *et al.*, "Preparation of environmentally friendly acrylic pressure-sensitive adhesives by bulk photopolymerization and their performance," *RSC Adv.*, vol. 10, no. 17, pp. 10277–10284, 2020, doi: 10.1039/C9RA10514J.
- [2] S. Sun, M. Li, and A. Liu, "A review on mechanical properties of pressure sensitive adhesives," *Int. J. Adhes. Adhes.*, vol. 41, pp. 98–106, Mar. 2013, doi: 10.1016/j.ijadhadh.2012.10.011.
- [3] N. Ballard, "Designing acrylic latexes for pressure-sensitive adhesives: a review," *Polym. Int.*, vol. 73, no. 2, pp. 75–87, Feb. 2024, doi: 10.1002/pi.6596.
- [4] C. I Gi, S. N. Gan, and D. T.-C. Ang, "Designing polymeric coating with low coefficient of friction for natural rubber glove application," *J. Ind. Eng. Chem.*, vol. 132, pp. 496–506, Apr. 2024, doi: 10.1016/j.jiec.2023.11.043.
- [5] M. R. Sanghvi, O. H. Tambare, and A. P. More, "Performance of various fillers in adhesives applications: a review," *Polym. Bull.*, vol. 79, no. 12, pp. 10491–10553, Dec. 2022, doi: 10.1007/s00289-021-04022-z.
- [6] Y. Wang, B. Sun, Z. Hao, and J. Zhang, "Advances in Organic–Inorganic Hybrid Latex Particles via In Situ Emulsion Polymerization," *Polymers (Basel)*., vol. 15, no. 14, p. 2995, Jul. 2023, doi: 10.3390/polym15142995.
- [7] R. Muthuraj, M. Misra, and A. K. Mohanty, "Biodegradable compatibilized polymer blends for packaging applications: A literature review," *J. Appl. Polym. Sci.*, vol. 135, no. 24, Jun. 2018, doi: 10.1002/app.45726.
- [8] L.-X. Zhang, J. Hu, Y.-B. Jia, R.-T. Liu, T. Cai, and Z. P. Xu, "Two-dimensional layered double hydroxide nanoadjuvant: recent progress and future direction," *Nanoscale*, vol. 13, no. 16, pp. 7533– 7549, 2021, doi: 10.1039/D1NR00881A.
- [9] C. Taviot-Guého, V. Prévot, C. Forano, G. Renaudin, C. Mousty, and F. Leroux, "Tailoring Hybrid Layered Double Hydroxides for the Development of Innovative Applications," *Adv. Funct. Mater.*, vol. 28, no. 27, Jul. 2018, doi: 10.1002/adfm.201703868.
- [10] K. F. Amin, Asrafuzzaman, A. M. Nahin, and M. E. Hoque, "Polymer nanocomposites for adhesives and coatings," in *Advanced Polymer Nanocomposites*, Elsevier, 2022, pp. 235–265. doi: 10.1016/B978-0-12-824492-0.00014-3.
- [11] E. Lizundia, V. A. Makwana, A. Larrañaga, J. L. Vilas, and M. P. Shaver, "Thermal, structural and degradation properties of an aromatic–aliphatic polyester built through ring-opening polymerisation," *Polym. Chem.*, vol. 8, no. 22, pp. 3530–3538, 2017, doi: 10.1039/C7PY00695K.
- [12] L. Wang, J. Wang, Y. Qi, F. Zhang, Z. Weng, and X. Jian, "Preparation of Novel Epoxy Resins Bearing Phthalazinone Moiety and Their Application as High-Temperature Adhesives," *Polymers (Basel).*, vol. 10, no. 7, p. 708, Jun. 2018, doi: 10.3390/polym10070708.
- [13] H. Sutar, B. Mishra, P. Senapati, R. Murmu, and D. Sahu, "Mechanical, Thermal, and Morphological Properties of Graphene Nanoplatelet-Reinforced Polypropylene Nanocomposites: Effects of Nanofiller Thickness," *J. Compos. Sci.*, vol. 5, no. 1, p. 24, Jan. 2021, doi: 10.3390/jcs5010024.
- [14] C. S. P. Borges, S. Jalali, P. Tsokanas, E. A. S. Marques, R. J. C. Carbas, and L. F. M. da Silva, "Sustainable Development Approaches through Wooden Adhesive Joints Design," *Polymers (Basel).*, vol. 15, no. 1, p. 89, Dec. 2022, doi: 10.3390/polym15010089.
- [15] L. E. Porath and C. M. Evans, "Importance of Broad Temperature Windows and Multiple Rheological Approaches for Probing Viscoelasticity and Entropic Elasticity in Vitrimers," *Macromolecules*, vol.

- 54, no. 10, pp. 4782-4791, May 2021, doi: 10.1021/acs.macromol.0c02800.
- [16] K.-Y. Hsiao, R.-J. Chung, P.-P. Chang, and T.-H. Tsai, "Identification of Hydroxyl and Polysiloxane Compounds via Infrared Absorption Spectroscopy with Targeted Noise Analysis," *Polymers (Basel).*, vol. 17, no. 11, p. 1533, May 2025, doi: 10.3390/polym17111533.
- [17] E. Casanova *et al.*, "The use of vibrational spectroscopy techniques as a tool for the discrimination and identification of the natural and synthetic organic compounds used in conservation," *Anal. Methods*, vol. 8, no. 48, pp. 8514–8527, 2016, doi: 10.1039/C6AY02645A.
- [18] R. M. Lees *et al.*, "Fourier transform spectroscopy of CH3OH: rotation–torsion–vibration structure for the CH3-rocking and OH-bending modes," *J. Mol. Spectrosc.*, vol. 228, no. 2, pp. 528–543, Dec. 2004, doi: 10.1016/j.jms.2004.06.004.
- [19] K. Wnuczek, A. Puszka, Ł. Klapiszewski, and B. Podkościelna, "Preparation, Thermal, and Thermo-Mechanical Characterization of Polymeric Blends Based on Di(meth)acrylate Monomers," *Polymers (Basel).*, vol. 13, no. 6, p. 878, Mar. 2021, doi: 10.3390/polym13060878.
- [20] S. Petrescu, M. Constantinescu, E. M. Anghel, I. Atkinson, M. Olteanu, and M. Zaharescu, "Structural and physico-chemical characterization of some soda lime zinc alumino-silicate glasses," *J. Non. Cryst. Solids*, vol. 358, no. 23, pp. 3280–3288, Dec. 2012, doi: 10.1016/j.jnoncrysol.2012.09.001.
- [21] M. Irfan *et al.*, "Arsenite [As(III)] Removal from Water Using Layered Double Hydroxide/Biochar Hybrid Composites: Synthesis, Characterization, and Reactive Site Identification," *Earth Syst. Environ.*, vol. 9, no. 3, pp. 1737–1753, Sep. 2025, doi: 10.1007/s41748-025-00751-7.
- [22] M. A. Muñoz, C. Carmona, and M. Balón, "FTIR study of water clusters in water-triethylamine solutions," *Chem. Phys.*, vol. 335, no. 1, pp. 37–42, May 2007, doi: 10.1016/j.chemphys.2007.03.015.
- [23] P. Szymoniak, Z. Li, D.-Y. Wang, and A. Schönhals, "Dielectric and flash DSC investigations on an epoxy based nanocomposite system with MgAl layered double hydroxide as nanofiller," *Thermochim. Acta*, vol. 677, pp. 151–161, Jul. 2019, doi: 10.1016/j.tca.2019.01.010.
- [24] W. Shu and I. Stanciulescu, "Fully coupled thermo-mechanical cohesive zone model with thermal softening: Application to nanocomposites," *Int. J. Solids Struct.*, vol. 188–189, pp. 1–11, Apr. 2020, doi: 10.1016/j.ijsolstr.2019.09.015.
- [25] M. J. Mochane, S. I. Magagula, J. S. Sefadi, E. R. Sadiku, and T. C. Mokhena, "Morphology, Thermal Stability, and Flammability Properties of Polymer-Layered Double Hydroxide (LDH) Nanocomposites: A Review," *Crystals*, vol. 10, no. 7, p. 612, Jul. 2020, doi: 10.3390/cryst10070612.
- [26] T. Hu *et al.*, "Layered double hydroxide-based nanomaterials for biomedical applications," *Chem. Soc. Rev.*, vol. 51, no. 14, pp. 6126–6176, 2022, doi: 10.1039/D2CS00236A.
- [27] Z. Gu, S. Li, F. Zhang, and S. Wang, "Understanding Surface Adhesion in Nature: A Peeling Model," Adv. Sci., vol. 3, no. 7, Jul. 2016, doi: 10.1002/advs.201500327.
- [28] S. M. Taghizadeh and D. Ghasemi, "Rheological and adhesion properties of acrylic pressure-sensitive adhesives," *J. Appl. Polym. Sci.*, vol. 120, no. 1, pp. 411–418, Apr. 2011, doi: 10.1002/app.33153.
- [29] R. Etemadi, B. Wang, K. M. Pillai, B. Niroumand, E. Omrani, and P. Rohatgi, "Pressure infiltration processes to synthesize metal matrix composites A review of metal matrix composites, the technology and process simulation," *Mater. Manuf. Process.*, vol. 33, no. 12, pp. 1261–1290, Sep. 2018, doi: 10.1080/10426914.2017.1328122.
- [30] J.-H. Lee, W. Zhang, H.-J. Ryu, G. Choi, J. Y. Choi, and J.-H. Choy, "Enhanced thermal stability and mechanical property of EVA nanocomposites upon addition of organo-intercalated LDH nanoparticles," *Polymer (Guildf).*, vol. 177, pp. 274–281, Aug. 2019, doi: 10.1016/j.polymer.2019.06.011.

KRONIKA JOURNAL(ISSN NO-0023:4923) VOLUME 25 ISSUE 10 2025

- [31] B. Nagendra, K. Mohan, and E. B. Gowd, "Polypropylene/Layered Double Hydroxide (LDH) Nanocomposites: Influence of LDH Particle Size on the Crystallization Behavior of Polypropylene," *ACS Appl. Mater. Interfaces*, vol. 7, no. 23, pp. 12399–12410, Jun. 2015, doi: 10.1021/am5075826.
- [32] Z.-D. Xu, T. Ge, and J. Liu, "Experimental and Theoretical Study of High-Energy Dissipation-Viscoelastic Dampers Based on Acrylate-Rubber Matrix," *J. Eng. Mech.*, vol. 146, no. 6, Jun. 2020, doi: 10.1061/(ASCE)EM.1943-7889.0001802.